Journal of Archaeological Science: Reports 23 (2019) 973–982

Contents lists available at ScienceDirect

Journal of Archaeological Science: Reports

journal homepage: www.elsevier.com/locate/jasrep

Demography and climate in Late Eneolithic Ukraine, Moldova, and Romania: Multiproxy evidence and pollen-based regional corroboration

Thomas K. Harper

Human Paleoecology and Isotope Geochemistry Lab, Department of Anthropology, Pennsylvania State University, 403 Carpenter Building, University Park, PA 16802, USA

ARTICLE INFO

Keywords:
Cucuteni-Tripolye culture
Modern analogue technique
Paleoclimate
Migrations
Demography
Ukraine
Romania

ABSTRACT

Attempts to correlate macro-scale climate dynamics with anomalies in local and regional archaeological data sets should account for differences in geographic scale and effect size. Using the modern analogue technique, this paper reconstructs temperature, precipitation, and growing degree-day trends in Ukraine, Moldova, and Romania from a set of 20 pollen cores in order to explicate the regional impact of the 6.0–5.0 ka BP rapid climate change interval observed in the GISP2 K^+ glacio-chemical sequence. Results are compared against a model of regional demographic development covering the time span of 6000–3000 BCE. This study indicates that, while macro-scale trends are discernible in Eastern Europe, climatic instability during the fourth millennium BCE was regionally variable and resultant demographic responses were highly targeted and heterogeneous in nature. A period of cooling ca. 3825–3650 cal BCE resulted in the fracturing of Eneolithic complexes in Romania and generally spurred adaptation to more mobile systems of settlement and subsistence. However, a contemporaneous alternative response involved large-scale migrations to peripheral regions, including the establishment of the Tripolye giant-settlements in Central Ukraine. The methods used illustrate the need for obtaining more proximate confirmation when applying large-scale climate processes to explanations of local and regional archaeological contexts.

1. Introduction

1.1. Background

Climate history in Holocene Europe is traditionally delineated according to the Blytt-Sernander sequence of pollen zones, consisting of the Preboreal (10,000–9000 BP), Boreal (9000–8000 BP), Atlantic (8000–5000 BP), Subboreal (5000–2500 BP), and Subatlantic periods (2500 BP to present; Welten, 1982). The temporal correspondence between these phases and archaeological epochs—the Mesolithic and the Boreal, the Neolithic and the Atlantic, the Bronze Age and the Subboreal—represents cultural and technological adaptation to climate change at the broadest scale.

Following a final cold period during the Terminal Pleistocene (the Younger Dryas, ~12.9–11.7 ka BP) Early Holocene temperatures increased dramatically. This period saw a massive revision of subsistence strategies as fauna that were previously restricted to limited refugia during the Ice Age expanded into deglaciated regions where deciduous forests were rapidly expanding (Jochim, 2011). A common view during the last thirty years held that the following Atlantic period was at times warmer than present, with the last interval of warmth being a "Mid-Holocene Climatic Optimum" ca. 6200–5300 BP (Folland et al., 1990). During this period average temperatures were assumed to have been 1–2 °C higher in mid-latitudes and 3–4 °C higher in upper latitudes. The correspondence between postulated warm periods during the Atlantic period and the expansion of Neolithic complexes in Europe led to the belief that these intervals represented comparative times of plenty for Neolithic agriculturalists.

Further studies of European paleoclimate have not corroborated the Climatic Optimum, demonstrating that it was far weaker and confined to a slight temperature anomaly in Northern Europe. Results from pollen-based reconstructions suggest that higher-than-modern summer temperatures were in fact offset by colder winter temperatures, leaving the macro-scale European "energy budget" largely unchanged since the beginning of the Holocene (Davis et al., 2003). Meanwhile, mid-latitude proxy data contradict the idea entirely, at least during the range of 6200–5300 BP, when it was prevailingly cooler and drier with widespread deglaciation leading to a disruption of North Atlantic currents and monsoon cycles. The most prominent result of these processes was the final desiccation of the Sahara and end of the "African Humid Period" (Bond et al., 1997).

E-mail address: tkh130@psu.edu.

http://dx.doi.org/10.1016/j.jasrep.2017.06.010
Received 31 March 2017; Accepted 10 June 2017
Available online 20 June 2017
2352-409X/

1.2. Rapid climate change

With the exception of present anthropogenic climate change, which may qualify as being severe enough to herald a new epoch (the "Anthropocene;" Waters et al., 2016), Holocene climate dynamics are now defined according to wide-ranging but brief "events," often under the monikers of rapid or abrupt climate change. High-resolution proxy datasets have allowed the explication of periodic variability in interwoven systems of solar radiation, deglaciation, ocean currents, air currents, and monsoon strength, as well as the effects of these systems on regional environments. During the 1990s, Gerard Bond and his colleagues, examining the prevalence of ice-rafted debris in North Atlantic sediments, established a roughly 1500-year cycle of climate change defined by eponymous Bond Events (Bond et al., 1997; Bond et al., 2008). Over the course of the Holocene, these events were identified at 11.1, 10.3, 9.4, 8.2, 5.9, 4.2, 2.8, 1.4, and 0.5 ka BP. The 8.2 ka event has become the most readily identifiable in European and Near Eastern archaeological literature owing to its manifestation in local datasets documenting tree ring and speleothem growth patterns, pollen ratios, and faunal proxies (Weninger et al., 2006, 2009).

Bond Events subsequently found confirmation in atmospheric data sets, leading to the separation of "atmospheric" and "oceanic" components of these climate change cycles. The GISP2 D (deep) ice core sodium (Na^+) and potassium (K^+) ion sequences (Mayewski et al., 1997) were found to be indicators of what Peter Mayewski and his colleagues (Mayewski et al., 2004) termed "Holocene rapid climate change" (RCC). The rate at which these ions were deposited in Greenlandic ice correlated with the strength of semi-permanent meteorological systems, the Icelandic Low and Siberian High pressure systems, respectively, the latter of which was extensively influential on Asian monsoon strength and Eurasian temperature and aridity. Based on the comparison of the GISP2 records with worldwide proxy data sets, Mayewski's team identified RCC intervals at roughly 9.0–8.0, 6.0–5.0, 4.2–3.8, 3.5–2.5, 1.2–1.0 and 0.6–0.1 ka BP (Fig. 1). While these do not correspond with Bond Events in every case, major RCC events seem to generally be preceded by a disruption in ocean circulation, which, after a slight lag, begins to disrupt atmospheric systems, namely the North Atlantic Oscillation (formed by the Icelandic Low and Azores High pressure systems).

Recent studies into Northern Hemisphere climate dynamics highlight the importance of thermohaline circulation, especially the Atlantic meridional overturning circulation (AMOC), in maintaining the prevailingly mild conditions in much of continental Europe. The AMOC weakened greatly over the course of the twentieth century due to the formation of a low-temperature subpolar gyre in the middle North Atlantic caused by melting of the Greenland ice sheet (Rahmstorf et al., 2015). Increasing meltwaters and continued weakening of the AMOC due to anthropogenic global warming are predicted for the future, with a 44% chance of total collapse ca. 2300 CE (Bakker et al., 2016). These studies illustrate the effects on circumpolar warming on ocean circulation and provide some observational corroboration for the mechanics of RCC in the paleoclimate record.

1.3. Climate of the fourth millennium BC

The latter part of the fourth millennium BCE witnessed the end of the Neo-Eneolithic complexes that defined European culture for approximately 3000 years, with the transition to Early Bronze Age archaeological assemblages completing ca. 3000 BCE. The climatic context of this transition was set by the 5.9 ka event (Bond Event 4), and the corresponding 6.0–5.0 ka RCC cycle. Concordance in proxy records suggests that the most acute period of climate change occurred during the first half of this interval (ca. 4100–3700 BCE), with the latter half characterized by comparatively moderate instability. This event roughly corresponds with the transition to the Subboreal period, and is characterized by cooler, drier conditions throughout much of the Old World.

Pertinent datasets for discussing the mechanics of RCC are the GISP2 K^+ sequence, proxy for Siberian High strength (Mayewski et al., 1997); the NGRIP $\delta^{18}O$ record, proxy for Northern Hemisphere temperature (NGRIP, 2004); the percentage of warm species encountered in Aegean Sea core LC21, proxy for sea surface temperature (SST) (Rohling et al., 2002); the rate of aeolian deposition in the Eifel Valley, Germany (Sirocko et al., 2005), proxy for Central European aridity; and North Atlantic Bond Event (ice rafted debris) data (Bond et al., 2008), a proxy for periodic pulses of glacial melt waters into the North Atlantic. Comparison of these proxy data with the Blytt-Sernander climate periodization and the overall archaeological "ages" shows the convergence of climatic and cultural transitions during the 6.0–5.0 ka RCC interval.

While discussions of macro-scale climate trends are by nature subject to varying dating resolution and several centuries of uncertainty, the progression of Bond Event 4 illustrates the lag time between oceanic events and atmospheric responses, with atmospheric climate in Europe not being seriously affected until a certain temperature threshold is reached and the AMOC is interrupted. The response in LC21 is slightly offset, indicating that it took some time before the effects of the Atlantic meltwater pulse were evident in the Mediterranean. Then, an early recovery of warm species at this site, during the period of maximal ice rafting ca. 3500 BCE, agrees with trends in the atmospheric proxies which seem to indicate an amelioration (though not cessation) of RCC conditions. The cause of this may be related to fluctuations in the position of the Intertropical Convergence Zone (ITCZ), a narrow convective strip positioned slightly north of the equator that (in the modern era) changes position seasonally, from 9°N in summer to 2°N in winter. ITCZ position does not seem to have much direct bearing on the RCC events identified by Mayewski and his colleagues, but the 5.9 ka event happens to coincide with a southerly shift in its position. This is associated with cooler temperatures in the Northern Hemisphere (Schneider et al., 2014). As the ITCZ resumed a more northerly average position over the course of the fourth millennium BC, conditions improved to some degree despite the ongoing disruption of the North Atlantic Oscillation.

On the global scale, the impact of the 5.9 event on human society was most pronounced in the mid-latitudes, where desertification prompted population agglomeration in river valleys and contributed to the rise of the first state-level societies (Brooks, 2006). Its influence on the archaeological cultures of Eastern Europe is less articulated, but researchers have discussed regional climate fluctuations (Anthony, 2007; Diachenko, 2010; Dolukhanov et al., 2009; Manzura, 2005) that in nearly all cases are manifestations of the same overall mechanism described here. The prospect of explicitly connecting the 5.9 ka event to Eastern Europe becomes clear given the synchronicity of its onset and two major demographic events: the abandonment of settlements belonging to the Gumelnița culture in the Danube Valley and the establishment of the Tripolye giant-settlements in Central Ukraine (Weninger and Harper, 2015).

Simple synchronicity of these events (e.g. the qualitative comparison of summed ^{14}C distributions and climate proxy data) does not establish causation, especially given vast differences in scale and data resolution. Lack of representation in the radiocarbon record does not necessarily indicate a lack of occupation; the later Eneolithic in particular represents a transition to generally more ephemeral upland settlements, sites that are radiometrically underrepresented in comparison to multilayer tells. Advances in demographic modeling based on the large-scale systematization of regional settlement data (Harper, 2016) create a proxy for human impacts that, in comparison with ^{14}C, is more complete, representative, and less prone to sampling bias (explained further in Section 2.3).

In the forest-steppe regions of Ukraine and Moldova, a well-developed relative typo-chronology suggests extensive long-distance influences and material exchange during the 6.0–5.0 ka interval, which were identified as being at least partially indicative of migrations

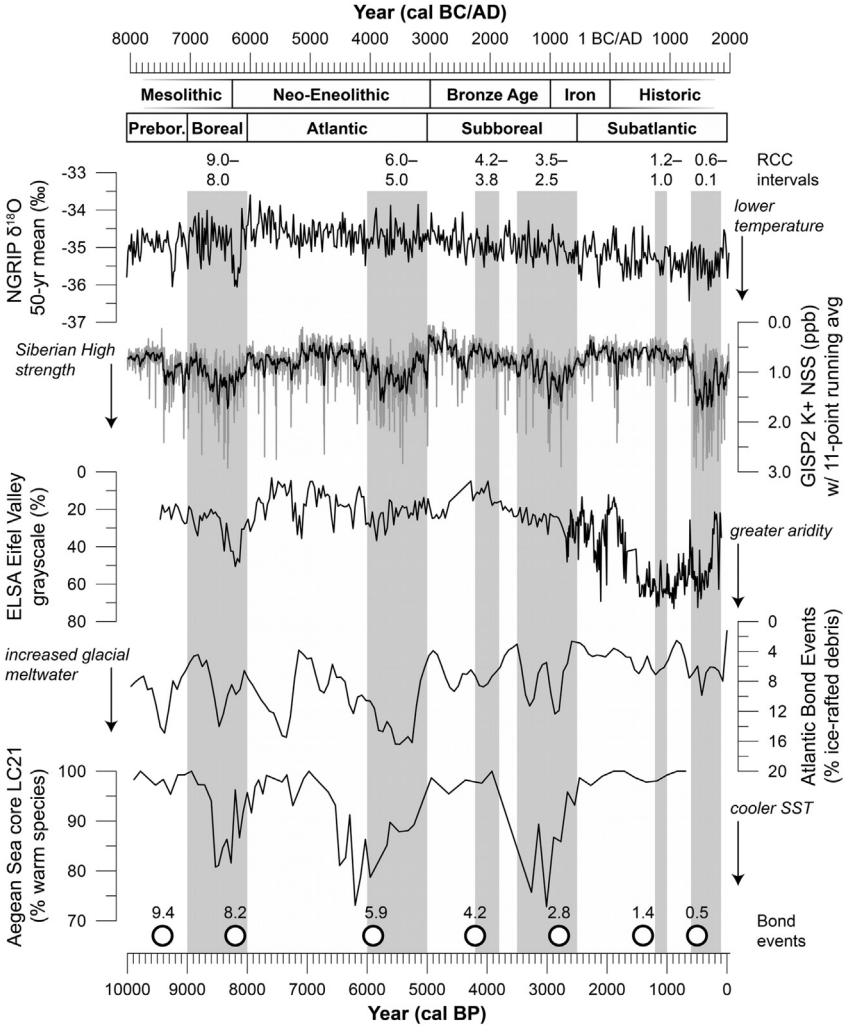

Fig. 1. Proxies for rapid climate change in Europe from 0 to 10 ka BP.

(Diachenko, 2010, 2012; Ryzhov, 1993, 1999, 2007a). Regional population reconstructions identify numerous periods where growth rates either exceeded the endogenous biotic potential or resulted in rapid population losses between one settlement generation and the next (Harper, 2016). While it is difficult to establish whether population growth in some areas was endogenous or migratory (likely both), rapid fluctuations in growth and the colonization of new territory appear to be responses to changing environment and, perhaps, increased conflict for subsistence resources (Dergachev, 2007; Harper, 2013).

2. Methods

2.1. The modern analogue technique

The most common, and deserved, criticism of directly comparing macro-scale climate trends and archaeological proxies is the disparity in their spatio-temporal scales. Climate systems have a highly dynamic and complex relationship with local and regional environments, and it is these smaller-scale impacts that dictated prehistoric subsistence and settlement patterns. It is necessary to establish which, if any, effects can be perceived on the micro-scale. The efficacy of pollen as a statistical indicator of ecology and climate change has been established since the beginnings of modern palynology, though tempered by the perennial considerations of differential preservation, downwash through sediment cores, and the effects of wind and weather on annual pollen distribution (Cain, 1939). Rather than illustrating an absolute picture of the environment at a given time reference, the utility of fossil pollen sequences lies in reconstructing general trends in vegetation cover and ecology.

This study utilizes the best modern analogue technique, particularly as it is implemented by Takeshi Nakagawa and his colleagues (Nakagawa et al., 2002). Using the Polygon 2.4.4 software environment (Nakagawa, 2016), it is possible to perform an automated empirical orthogonal function (EOF) analysis, which examines variation in multiple dimensions and outputs reconstructed time series and error estimates based on the similarity between a fossil pollen sample and modern sites for which meteorological measurements are known.

Taxa were grouped on the basis of plant functional types (PFT), categories that describe the generalized morphology, phenology, and climatic thresholds of plants. PFTs can be thought of taxonomically as the constituent plant classes of biomes (Prentice et al., 1996), and their statistical validity as climatic indicators is well-established (Peyron et al., 1998; Prentice et al., 1996; Nakagawa et al., 2002). This study examines 106 pollen taxa grouped into 25 PFTs derived from previous studies of Eurasian biomes and paleoclimate (Peyron et al., 1998; Prentice et al., 1996; Tarasov et al., 1998; Table 1). While the modern analogue algorithm employed by Polygon is indifferent to the method of plant classification, the use of PFTs simplifies computation by reducing the number of variables and therefore the number of EOF axes.

In order to perform each reconstruction, three data sets with a unified categorization must be input into the software environment. A reference set of 4826 modern surface pollen samples was assembled based on the European Modern Pollen Database (EMPD v3; Davis, 2016; Davis et al., 2013; see Fig. 2). Climate data for each set of surface

Table 1
Pollen taxa and PFT assignments.

Taxa	PFT name	Code
Betula nana, *Dryas*, *Pedicularis*, *Rhododendron*, *Saxifraga*, *Vaccinum*	Arctic-alpine dwarf shrub	aa
Picea, *Pinus* subgen. *Strobus* (Haploxylon)	Boreal evergreen conifer	bec
Abies	Boreal evergreen/cool-temperate conifer	bec/ctc
Betula, *Larix*, Liliaceae	Boreal summergreen	bs
Alnus viridis	Boreal summergreen/arctic-alpine	bs/aa
Cornus, *Sambucus*, *Sorbus*, *Viburnum*	Boreal-temperate summergreen shrub	bts
Hippophae, *Polygonum*	Cold grass shrub	cgs
Buxus, *Hedera*, *Ilex*	Cool-temperate broad-leafed evergreen	wte1
Carpinus, *Corylus*, *Fagus*, *Frangula*, *Tilia*, *Ulmus/Zelkova*	Cool-temperate summergreen	ts1
Ephedra	Desert forb/warm grass shrub	df/wgs
Juniperus, *Pinus* subgen. *Pinus* (Diploxylon)	Eurythermic conifer	ec
Poaceae/Gramineae	Grass	g
Calluna, *Empetrum*, Ericaceae	Heath	h
Cedrus, *Taxus*	Intermediate temperate conifer	ctc1
Cyperaceae	Sedge	s
Artemisia	Steppe forb/desert forb	sf/df
Allium, Amaranthaceae/Chenopodiaceae, Apiaceae/Umbelliferae, *Armeria*, Asteraceae/Compositae, Boraginaceae, Campanulaceae, Cannabaceae, Caryophyllaceae, *Centaurea*, Convolvulaceae, Dipsacaceae, *Epilobium*, Euphorbiaceae, *Filipendula*, *Galium*, Geraniaceae, *Helianthemum*, Iridaceae, Lamiaceae/Labiatae, Onagraceae, Papaveraceae, *Plantago*, Plumbaginaceae, *Potentilla*, Ranunculaceae, Rosaceae, Rubiaceae, *Sanguisorba*, *Scabiosa*, *Stellaria*, *Taraxacum*, *Thalictrum*	Steppe forb/shrub	sf
Polygonaceae, Scrophulariaceae, Valerianaceae	Steppe/arctic-alpine forb	sf/aa
Acer, *Fraxinus* subgen. *Fraxinus*, *Quercus* (Deciduous)	Temperate summergreen	ts
Populus	Temperate/boreal summergreen	bs/ts
Alnus, *Salix*	Temperate/boreal summergreen/arctic-alpine	bs/ts/aa
Brassicaceae/Cruciferae, Crassulaceae, Fabaceae/Leguminosae, *Zizyphus*	Warm grass shrub	wgs
Quercus (Evergreen)	Warm-temperate broad-leafed evergreen	wte
Acacia, *Ceratonia*, Cistaceae, *Myrtus*, *Olea*, *Phillyrea/Fontanesia*, *Pistacia*, *Rhus*	Warm-temperate sclerophyll tree/shrub	wte2
Castanea, *Fraxinus* subgen. *Ornus*, *Juglans*, *Myrica*, *Ostrya/Carpinus Orientalis*, *Platanus*, Rhamnaceae, *Vitis*	Warm-temperate summergreen	ts2

pollen coordinates were then extracted in QGIS from the 30-min CRU Global Climate Dataset distributed by the Intergovernmental Panel on Climate Change (Mitchell et al., 2004; Mitchell and Jones, 2005). These data sets are organized into 30-year averages, with 1961–1990 constituting the modern baseline. Finally, the fossil pollen data were prepared and analyzed. Along with the reference data, the process of cleaning and preparing these data sets is by far the most labor intensive aspect of the modern analogue approach, requiring the manual organization and systematization of hundreds or thousands of taxa.

For each time reference within a fossil pollen data set, the closest modern analogues are computed based on either the measured proportions of pollen taxa or the EOF chord distance, with the precision of the reconstruction varying based on the number of analogues chosen as well as an "envelope" value. The number of analogues may range from 1 to 20, with the default being eight. With greater numbers of analogues the model precision decreases but accuracy increases, while fewer analogues will produce a more precise time series but with far greater error. The envelope controls the definition of how "tight" analogue affinity must be, which is then defined by a multi-dimensional convex hull; the closest analogues, up to the maximum number defined, are then selected from this region.

The reconstructions explored here use seven EOF axes, representing a total of 82.203% of variation. PFT proportions are used to define the chord distance between samples, which is left unweighted. Minor taxa

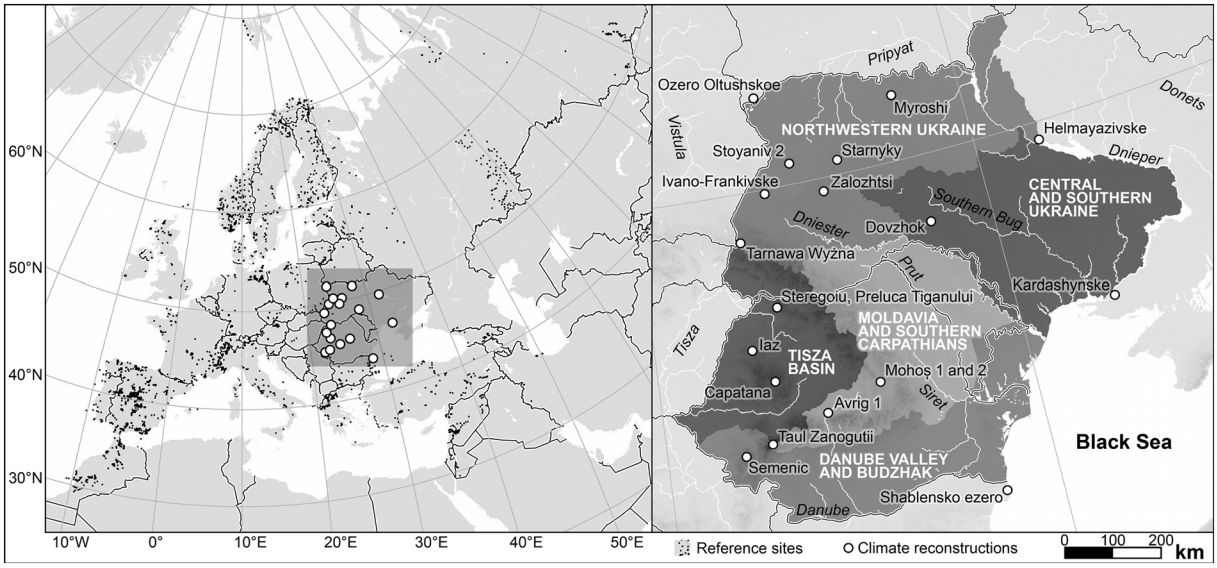

Fig. 2. Left – location of reference sample locations from the EMPD. Right – location of climate reconstruction sites and analytical regions within the study area.

Table 2
Characteristics of pollen cores used in the analysis.

Site	Lat	Long	Elevation (m asl)	Temporal range (ka BP)	Mean res. (yrs)	Age-depth model	Representative studies
Danube Valley and Budzhak							
Shablensko ezero	43.58	28.55	12	0.5–9.6	233	Cal BP linear	Filipova, 1985
Semenic	45.18	22.06	1408	0.0–10.9	139	EPD cal BP	Rösch and Fischer, 2000
Central and Southern Ukraine							
Dovzhok	48.75	28.25	273	0.2–8.7	177	EPD cal BP	Kremenetski, 1995
Helmayazivske	49.82	31.86	80	0.3–9.2	524	Cal BP linear	Artyushenko et al., 1982a
Kardashynske	46.52	32.62	−1	0.2–9.4	245	EPD cal BP	Kremenetski, 1995
Moldavia and Southern Carpathians							
Avrig 1	45.72	24.38	383	0.0–19.6	130	EPD author	Tantau, 2003
Mohoș 1	46.08	25.92	992	0.0–12.4	62	EPD cal BP	Tantau, 2003
Mohoș 2	46.08	25.92	992	0.1–9.0	82	EPD cal BP	Tantau, 2003
Northwestern Ukraine							
Ivano-Frankivske	49.92	23.77	294	0.4–13.1	354	Cal BP linear	Artyushenko et al., 1982b
Myroshi	51.20	28.00	192	0.1–9.0	415	Cal BP linear	Chernavskaya and Fogel, 1989
Ozero Oltushskoe	51.70	23.96	156	0.4–11.6	268	Cal BP linear	EPD; Y.K. Yelovicheva
Starnyky	50.27	26.02	262	0.4–13.7	442	Cal BP linear	Bezusko et al., 1985
Stojaniv 2	50.38	24.63	237	0.2–8.2	286	Cal BP linear	Bezusko et al., 1988
Tarnawa Wyżna	49.10	22.83	699	2.7–14.1	181	Cal BP linear	EPD; M. Ralska-Jasiewiczowa
Zalozhtsi	49.75	25.45	335	0.3–9.9	402	Cal BP linear	Bezusko et al., 1988
Tisza Basin							
Capatana	46.47	23.14	1189	0.2–7.6	85	EPD cal BP	Farcas et al., 2003
Iaz	47.11	22.66	319	0.0–17.4	60	EPD cal BP	Grindean et al., 2014
Preluca Tiganului	47.82	23.54	710	0.1–14.3	63	Cal BP linear	Feurdean and Bennike, 2004
Steregoiu	47.81	23.54	853	0.0–17.4	68	EPD cal BP	Björkman et al., 2003
Taul Zanogutii	45.33	22.80	1860	0.1–22.2	175	EPD cal BP	Farcas et al., 1999

are not enhanced for outlier detection but are enhanced for climate reconstruction, reflecting the ability of less prevalent PFTs to be indicators for certain climate regimes. For every fossil pollen sample, reconstruction results are taken from the closest eight analogues; the large sample size of the reference set enabled the identification of numerous analogues even with a tight envelope value (0.2).

2.2. Pollen core and climate data

Fossil pollen data were obtained from the European Pollen Database (EPD; http://www.europeanpollendatabase.net). Selection criteria dictated that suitable cores must 1) have an extant age-depth model or ^{14}C data from which one may be constructed, and 2) have some level of coverage for the period of ~8000–5000 cal BP. Nineteen cores were ultimately selected; one each from Bulgaria, Belarus, and Poland, eight from Romania, and eight from Ukraine. Characteristics related to the coverage and resolution of these cores are summarized in Table 2.

Data are organized into five regions delineated by biogeographic and cultural boundaries (Fig. 2): the Danube Valley and Budzhak, the Tisza Basin, Moldavia and the Southern Carpathians, Northwestern Ukraine, and Central and Southern Ukraine.

When possible, preexisting age-depth models are used. However, calibrated ^{14}C results were not available for greater than half of the reconstructed cores, necessitating the construction of new age estimates for fossil pollen samples. Radiocarbon ages are determined using the IntCal 13 Northern Hemisphere curve (Reimer et al., 2013) and age-depth models assembled by linear interpolation in Paleontological Statistics (PAST) v 3.14 (Hammer, 2016).

Climate reconstructions focus on the three variables of mean annual temperature (MAT), mean annual precipitation (MAP), and growing degree-days (GDD). In each case these are computed from the monthly average data extracted from the CRU data sets. Reconstructed climate parameters were well-correlated with the modern data (R_{MAT} = 0.94; R_{MAP} = 0.84; R_{GDD} = 0.90) and mirror previous observations regarding the generally stronger relationship between pollen proportions and temperature as opposed to precipitation (Nakagawa et al., 2002).

Because of its direct effect on the maturation and productivity of crops, GDD stands as the most meaningful variable to compare with the population dynamics of sedentary agriculturalists. A variety of cereals and pulses were cultivated by Neo-Eneolithic peoples in eastern and southeastern Europe, but the most common cereal known from paleobotanical assemblages in Ukraine is emmer wheat, *Triticum dicoccum* (Pashkevich and Videjko, 2006). Emmer cultivation is rare today, but its ancestral status to modern durum wheat results in fairly consistent physiological properties between these species, which are often categorized as subspecies of *Triticum turgidum* rather than as discrete species.

Estimates for the growing degree-days necessary for wheat maturation vary considerably depending on the species and environmental context. Most modern estimates, while not usually explicitly stated, are derived for *Triticum aestivum* (common, or bread wheat). Bread wheat may be cultivated either in “winter” or “spring” varieties, named according to the season in which they are sown, but historical attestations of winter sowing practices indicate that it was most likely a relatively recent innovation that had no bearing on European Neolithic societies. Estimates for growing degree-days necessary for spring wheat maturation include 1624–1669 (Acevedo et al., 2002), 1538–1665 (Miller et al., 2001), and 1825 (Loper, 2012; NDAWN, 2002). Given that *Triticum aestivum* is descended from spelt hybridization and is more cold-tolerant than durum and emmer, the higher end of these estimates is justified in a prehistoric context and 1825 GDD is taken as a “vulnerability threshold” for Neo-Eneolithic subsistence systems. In order to germinate, wheat seeds require a temperature range of 4–37 °C, with 12–25 °C representing the most ideal range (Acevedo et al., 2002). This study follows the methods of Spinoni et al. (2015) in adopting a 5.5 °C base value and estimating GDD from gridded monthly temperature values.

2.3. Demographic data

Population history of Neo-Eneolithic Ukraine, Moldova, and Romania is reconstructed using a derivative of *SARP*, a settlement archaeology model that examines the number of settlements, their area, the number of rooms/houses per settlement, and the presumed

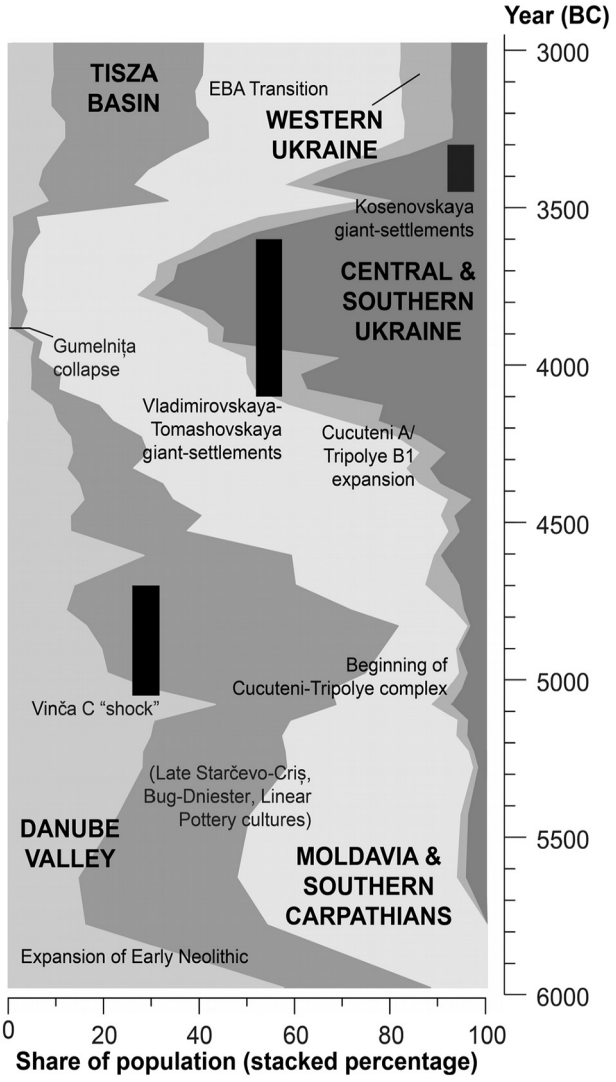

Fig. 3. Diachronic distribution of population in the study area in comparison with major archaeological events.

population density at a given time reference (Ammerman et al., 1976). In this case *R* and *P* are omitted due to the incomplete and conjectural nature of these data through much of the study area (with complete housing data available for only 1.5% of settlements), so the final product is a measure of synchronous hectares of settlement rather than an attempt at presenting "actual" population values. However, in those cases were data are available, it should be noted that settlement size was highly correlated with the number of structures ($r = 0.95$; $p < 0.001$).

Methodological developments over previous implementations of *SARP* include a large sample size ($n = 8072$), a unified 39-phase system of chronological classification that incorporates both relative and absolute chronology, and a computational component that imputes chronology and population data for data-deficient areas. The functioning of this model and its chronological basis are discussed in far greater detail in Harper, 2013 and Harper, 2016. Inter-regional population trends compare favorably with longstanding archaeological assumptions of demographic change accompanying major shifts in settlement and material culture (Fig. 3). While the primary focus of this paper concerns the last 1000 years of the Neo-Eneolithic, it bears mentioning that the model illustrates the general diffusion of the Neolithic as well as corroborating the Vinča C "shock" in Transylvania at the beginning of the Eneolithic (Lazarovici, 1987).

3. Results and discussion

3.1. General trends and RCC confirmation

All data sets were processed into justified time series of 50-year moving averages. Meaningful relationships between variables are then discerned in two ways: via sinusoidal curve fitting and cross-correlation analysis. Data extend from 4.5–8.5 ka, corresponding roughly with the Middle Holocene and Neo-Eneolithic and encompassing both the 8.2 and 5.9 ka events. On the level of the overall study area, reconstruction results closely resemble the trends obtained for Eastern Europe by Davis et al. (2003), using a similar data set but a different implementation of the modern analogue technique.

The periodicity of RCC events during the 4.5–8.5 ka window was analyzed using the sum-of-sinusoids function in PAST. Generalized over the Holocene, RCC cycles have a periodicity of ~1450 years (Mayewski et al., 1997), and this periodicity is confirmed here. With the GISP2 K^+ sequence as a baseline, there is a 1450-year interval between the 9.0–8.0 ka and 6.0–5.0 ka cycles, with a 2500-year interval between peak amplitudes. Including a further 4000-year component (the window width) allows the fitted curve to account for variations in amplitude between the two climate change intervals. Table 3 presents the results of this curve-fitting. In order to verify the validity of the fitted model, it is necessary to also examine cross-correlations between variables, which has the added benefit of showcasing the lag between the perceived onset of macro-scale climate events and regional environmental impacts.

MAT, MAP, and GDD values are averaged across the 20 pollen-based reconstructions to show general regional trends (Fig. 4). The goodness of fit (R^2) and cross-correlation values are adversely affected by the high (50-year) sampling resolution, so in this context the majority of results are deemed a moderate to excellent fit. A notable exception is the NGRIP $\delta^{18}O$ record which seems to be more weakly associated with RCC, though it correlates with pollen-based reconstructions on a level comparable to GISP2 (~0.3–0.4). This is to be expected since $\delta^{18}O$ is a commonly cited proxy for temperature and aridity, and the NGRIP record in particular is a famous indicator of the 8.2 ka event. It seems probable that a temperature anomaly detected here ca. 7950–7700 cal BP is actually this event, offset by several centuries due to chronological uncertainty.

3.2. Regional results and human impacts

Turning first to Romania and Moldova, the 5.9 ka event is perceptible within a lag time of approximately 100–300 years (Fig. 5). Demographic upheaval is evident throughout both countries, manifested

Table 3
Sinusoidal curve-fitting results and cross-correlations between RCC proxies and pollen-based reconstructions.

Proxy record	Sinusoidal fit R^2	*p*-Value	Peak cross-correlation with GISP2 K^+	*p*-Value	Lag time (yrs)
GISP2 K^+ NSS	0.65	< 0.0001	N/A	N/A	N/A
GISP2 Na + NSS	0.52	< 0.0001	0.56	< 0.0001	0
ELSA Eifel Valley	0.52	< 0.0001	0.55	< 0.0001	− 150
LC21	0.85	< 0.0001	− 0.61	< 0.0001	450
NGRIP $\delta^{18}O$	0.24	0.0014	− 0.32	0.0040	− 150
Bond Events	0.51	< 0.0001	0.62	< 0.0001	100
MAT	0.41	< 0.0001	− 0.34	0.0027	− 150
MAP	0.54	< 0.0001	0.43	< 0.0001	150
GDD	0.50	< 0.0001	− 0.46	< 0.0001	0

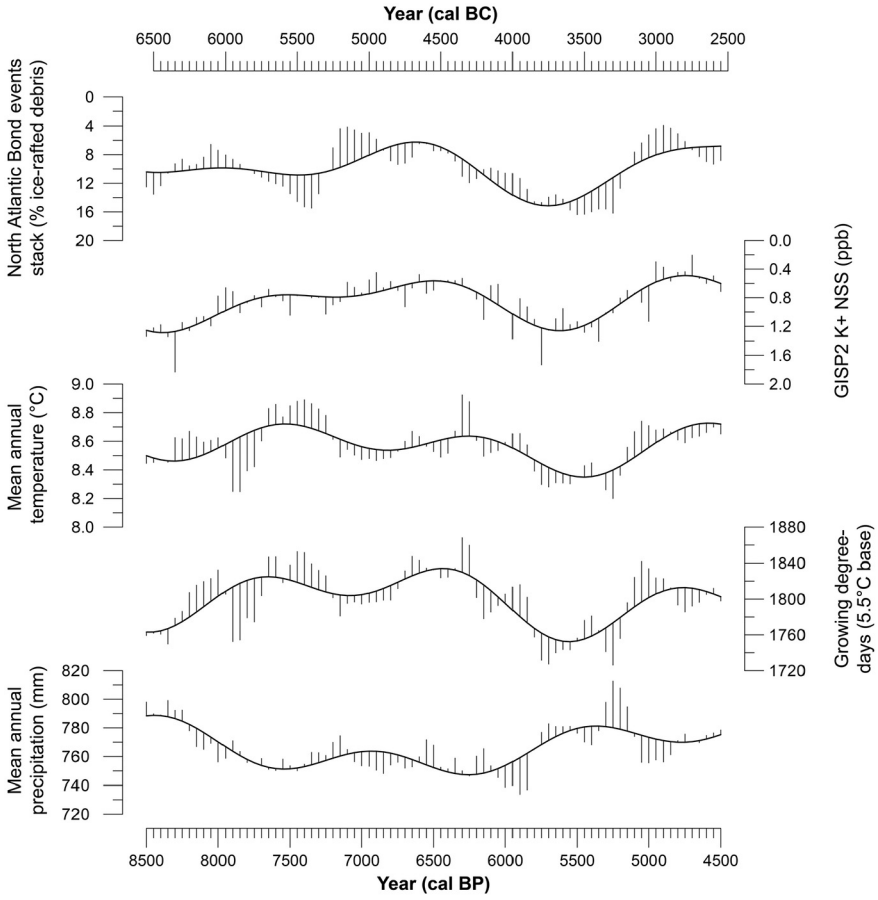

Fig. 4. Plot of sinusoidal fits and residuals for selected macroscale proxies (Bond Events, GISP K + NSS) and pollen based MAT, GDD, and MAP reconstructions. Data adhere closely to the 1450-year periodicity defined for RCC cycles.

in Transylvania by the end of the Tiszapolgár culture, in the Danube Valley by the collapse of Gumelnița tell settlements, and in Moldavia by the end of Cucuteni A-B and B1 and beginning of Cucuteni B2 (roughly contemporaneous with the beginning of Tripolye C1 in Moldova and Ukraine). Crucially, growing degree-days synchronously cross the vulnerability threshold at ca. 3825–3650 cal BC. Constraints on cereal maturation would have in turn limited the carrying capacity of settlement systems in Transylvania and Moldavia, regions with less productive soils than the rich fluvial environment of the Danube.

The Danube Valley is one case in which reliance on regional or super-regional proxies obscures variation, as the GDD reconstruction from Shablensko ezero on the Black Sea littoral (northeastern Bulgaria) indicates a much longer growing season than upland Romania. Throughout the fourth millennium BC, degree-days here fall in the range of 2200–2400. Evidence from the Austrian Alps indicates glacial recession at 4000–3600 BCE (Joerin et al., 2006), and these meltwaters would have flowed directly into the Danube catchment. At the river's mouth, meanwhile, optical luminescence dating places the formation of the St. George I lobe, the first stage in the accumulation of the modern Danube Delta, to slightly after this time (5210 ± 280 BP; Giosan et al., 2006). While it is tangential to this study, the Vinča C "shock" at the beginning of the fifth millennium BCE partially coincides with a similar (though less sustained) deglaciation event, and may illustrate a pattern of flood vulnerability for settlements in the Danube Valley.

Some of the populations represented by the Tiszapolgár or Gumelnița settlements were integrated into smaller successor groups (e.g. the Bodrogkeresztúr and Cernavodă 1c cultures), but most were likely absorbed into neighboring groups. Very little can be said about changes in vital statistics at this time due to a prevailing lack of human remains, but settlement data indicate that the overall population of Romania, Moldova, and Ukraine continued to grow for several centuries after the onset of the 5.9 ka event (mostly in Central Ukraine). David Anthony (2007) describes Gumelnița "refugees" merging with the Cucuteni-Tripolye complex and it seems to be the case that extensive contacts existed between the Cucuteni and Gumelnița cultures, with substantial exchange occurring during the periods of Cucuteni A and A-B (Mantu, 1998).

The population increase observed during Cucuteni A–B and B1 is of sufficient magnitude to accommodate excess population from the Danube and Tisza regions; given the temporal uncertainties inherent in both the demographic and climate modeling, it is plausible that some amount of these displaced peoples moved to Moldavia and contributed to this peak. This, in turn, exacerbated competition for resources in an already crowded region and encouraged the migratory pulses to peripheral regions that define the development of the Middle-Late Tripolye culture.

In opposition to Romania and Moldova, the onset of the 5.9 event is a time of unprecedented population growth in Ukraine, despite prevailingly less advantageous growing conditions (Fig. 6). The key distinctions between these two contexts are population density and resource competition; the colder temperatures and shorter growing season of Ukraine are offset by an initially negligible population density and an abundance of territory for settlement.

The early, prominent peak observed in Northwestern Ukraine is representative of widespread settlement in the Upper Dniester region at the interface of Tripolye B1–2 and B2/C1, the Zaleshchitskaya and early Shypenetskaya local groups. From a typological perspective, S.N. Ryzhov (2007b) states that Shypenetskaya influence is evident in the foundation of the Nebelevskaya giant-settlements of Central Ukraine, which occupy the middle (ca. 3950–3750 BCE) of the Vladimirovskaya-Tomashovskaya local group sequence. This ephemeral peak may be representative of serial migration; first from the Prut valley in Moldavia to the Upper Dniester, then to the area of the Southern Bug in Central Ukraine.

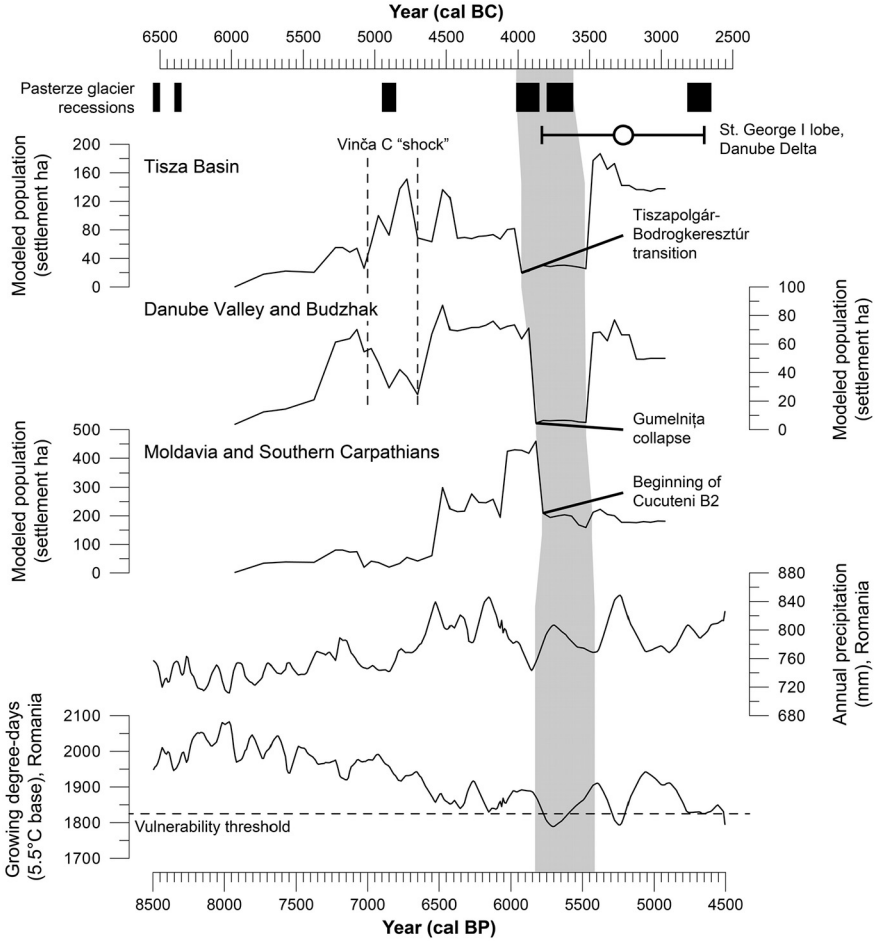

Fig. 5. Comparison of population trends in Romania and Moldova with precipitation and growing degree-day reconstructions and evidence for possible flooding in the Danube Valley.

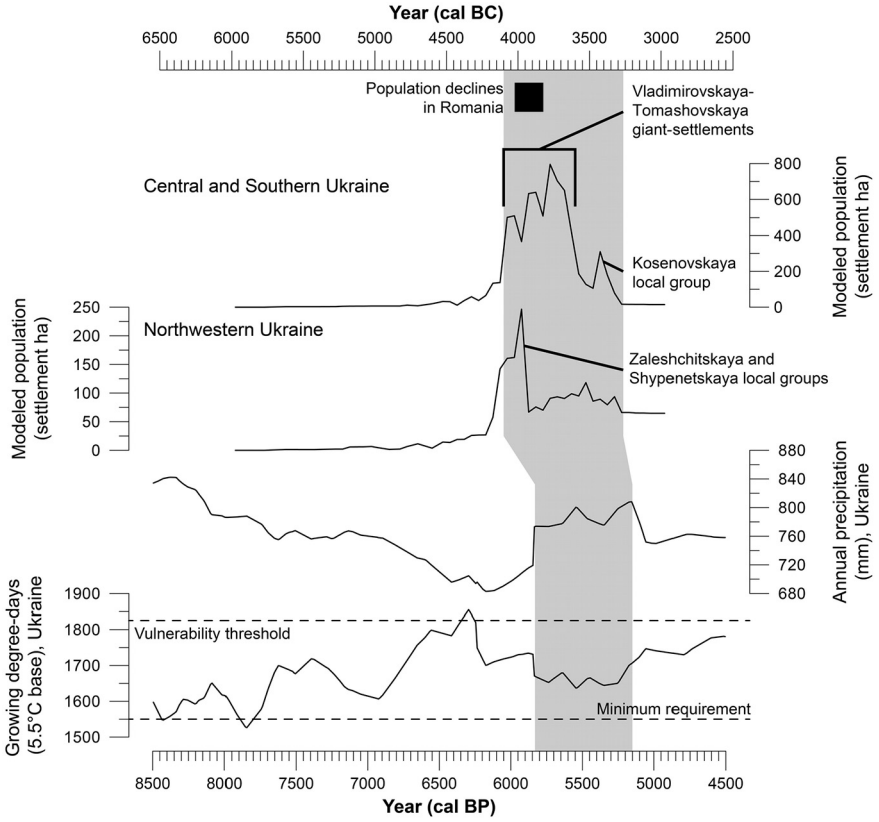

Fig. 6. Comparison of population trends in Ukraine with precipitation and growing degree-day reconstructions.

In the overall population history of the Neo-Eneolithic, the Tripolye giant-settlements (at 100–320 ha each) stand in stark contrast to the vast majority of systems based on local clusters of small and medium-sized sites, with median settlement size fluctuating between 0.5 and 4 ha (Harper, 2016). Their typological affinities, short period of habitation, and formation during a time of climatic degradation suggests that the giant-settlements were more a migratory reaction to events in the Cucuteni-Tripolye "core" area than an endogenous development (Diachenko, 2012; Harper, 2016).

3.3. Conclusion

While there is some ambiguity about the precise timing and nature of population movements around the time of the 5.9 ka event, its disruptive effect on demography in Eastern Europe is evident. Modeled growth trends are roughly sigmoidal during the Early to Middle Eneolithic, generally adhering to the Malthusian assumption of growth limited by carrying capacity. Population in the Tisza Basin and Danube Valley plateaued by the Early Eneolithic and Moldavia by the Middle Eneolithic. While small-scale networks of settlement and exchange existed in Ukraine as far back as the Early Neolithic, the major population growth beginning ca. 4100 BCE is almost entirely influenced by conditions in Romania and Moldova. The phenomenon of sudden population agglomeration in Central Ukraine during Tripolye B2 and C1 is consistent with recurrent, short-lived "false urbanization" of recent migrant populations within single sites (Diachenko, 2012).

The Eneolithic migratory vector to the forest-steppe region of Ukraine follows population density-dependent assumptions (as influenced by dynamic carrying capacity) and agrees with Manzura's (2005) characterization of a "steppe valve" to the east opening during times of crisis. Interestingly, within 500 years of RCC onset population values in Romania recovered to levels at or above those of the Early Eneolithic, while in Central and Southern Ukraine settlement nearly ceases. This is largely a result of changing socioeconomic regimes, with the succeeding Terminal Eneolithic groups being far more itinerant and prefiguring the arrival of EBA groups from the Eurasian steppe. The widespread movement and blending of Terminal Eneolithic assemblages into common "horizons" seems to indicate that the economic shift to itinerant pastoralism diagnostic of the EBA predated the large-scale arrival of populations from the Eurasian steppe, as represented by Yamnaya and Globular Amphora archaeological cultures.

The convergence and divergence of demographic and climatic trends in Eastern Europe at different time references invites many archaeological interpretations that cannot be visited in depth here. However, this study highlights a few major examples, while exploring aspects of regional variability that are crucial for establishing the influence of climate on smaller-scale phenomena. The inclusion of growing degree-day reconstructions, in particular, is put forward as a useful metric for evaluating the vulnerability of subsistence systems reliant on agronomic crops.

Acknowledgements

This research did not receive any specific grant from funding agencies in the public, commercial, or not-for-profit sectors.

References

Acevedo, E., Silva, P., Silva, H., 2002. Wheat growth and physiology. In: Curtis, B.C., Rajaram, S., Gómez Macpherson, H. (Eds.), Bread Wheat: Improvement and Production. FAO Plant Production and Protection Series 30 FAO, Rome.

Ammerman, A.J., Cavalli-Sforza, L.L., Wagener, D.K., 1976. Toward the estimation of population growth in old world prehistory. In: Zubrow, E.B.W. (Ed.), Demographic Anthropology: Quantitative Approaches. University of New Mexico Press, Albuquerque, pp. 27–62.

Anthony, D.W., 2007. The Horse, the Wheel, and Language: How Bronze-Age Riders From the Eurasian Steppes Shaped the Modern World. Princeton University Press, Princeton.

Artyushenko, A.T., Arap, P.Ya., Bezusko, L.G., Ilves, E.O., Kayutkina, T.M., Kovalyukh, N.N., 1982a. (in Russian) Novye dannye o rastitelnosti Ukrainy v golotsene [New data on the Holocene vegetation of Ukraine]. In: Velichko, A.A. (Ed.), Razvitie prirody territorii SSSR v pozdnem plejstotsene i golotsene. Nauka, Moscow, pp. 173–186.

Artyushenko, A.T., Arap, P.Ya., Bezusko, L.G., 1982b. (in Russian) *Istoriya rastitelnosti zapadnykh oblastej Ukrainy v chetvertichnom periode* [Vegetation History of the Western Oblasts of Ukraine during the Quaternary Period]. Naukova dumka, Kiev.

Bakker, P., Schmittner, A., Lenaerts, J.T.M., Abe-Ouchi, A., Bi, D., van den Broeke, M.R., Chan, W.-L., Hu, A., Beadling, R.L., Marsland, S.J., Mernild, S.H., Saenko, O.A., Swingedouw, D., Sullivan, A., Yin, J., 2016. Fate of the Atlantic Meridional Overturning Circulation: strong decline under continued warming and Greenland melting. Geophys. Res. Lett. 43 (23), 12252–12260.

Bezusko, L.G., Kayutkina, T.M., Kovalyukh, N.N., Artushenko, A.T., 1985. (in Ukrainian) Paleobotanichni ta radiokhronologichni doslidzhennya vidkladiv Starnyky (Male Polissya) [Paleobotanical and radiochronological study of sediments at Starniki (Male Polessie)]. Ukrainskyi Botanichnyi Zhurnal 42, 27–30.

Bezusko, L.G., Klimanov, V.A., Shelyag-Sosonko, Yu.R., 1988. (in Russian) Klimaticheskie usloviya Ukrainy v pozdnelednikove i golotsene [Climatic conditions of Ukraine in the Late Glacial and Holocene]. In: Khotinskij, N.A., Klimanov, V.A. (Eds.), Paleoklimaty golotsena Evropejskoj territorii SSSR. Mosow, IGAN SSSR, pp. 125–135.

Björkman, L., Feurdean, A., Wohlfarth, B., 2003. Late-Glacial and Holocene forest dynamics at Steregoiu in the Gutaiului Mountains, Northwest Romania. Rev. Palaeobot. Palynol. 124, 79–111.

Bond, G., Showers, W., Cheseby, M., Lotti, R., Almasi, P., deMenocal, P., Priore, P., Cullen, H., Hajdas, I., Bonani, G., 1997. A pervasive millennial-scale cycle in North Atlantic Holocene and glacial cycles. Science 278, 1257–1266.

Bond, G., et al., 2008. North Atlantic Holocene drift ice proxy data. In: IGBP PAGES/World Data Center for Paleoclimatology Data Contribution Series #2008-018. NOAA/NCDC Paleoclimatology Program, Boulder CO, USA.

Brooks, N., 2006. Cultural responses to aridity in the Middle Holocene and increased social complexity. Quat. Int. 151, 29–49.

Cain, S.A., 1939. Pollen analysis as a paleo-ecological research method. Bot. Rev. 5 (12), 627–654.

Chernavskaya, M.M., Fogel, G.A., 1989. (in Russian) Izmenchivost klimata yugo-zapada evropejskoj chasti SSSR v golotsene [Holocene climate variability in the southwestern part of the European USSR]. Dokl. Akad. Nauk SSSR 307 (6), 1474–1477.

Davis, B.A.S., 2016. The European Modern Pollen Database (EMPD) project Stage 2. http://www.europeanpollendatabase.net/wiki/doku.php?id=empd_database accessed 12.03.17.

Davis, B.A.S., Brewer, S., Stevenson, A.C., Guiot, J., 2003. The temperature of Europe during the Holocene reconstructed from pollen data. Quat. Sci. Rev. 22, 1701–1716.

Davis, B.A.S., Zanon, M., Collins, P., et al., 2013. The European Modern Pollen Database (EMPD) project. Veg. Hist. Archaeobotany 22, 521–530.

Dergachev, V.A., 2007. (in Russian) *O skipetrakh, o loshadyakh, o vojne: Etyudy v zashchitu migratsionnoj kontseptsii M. Gimbutas* [Of Scepters, Horses, and War: Studies in Support of the Migration Concept of M. Gimbutas]. Nestor-Istoriya, Saint Petersburg.

Diachenko, A.V., 2010. (in Russian) Evstaticheskie kolebaniya urovnya Chernogo morya i dinamika razvitiya naseleniya kukuten-tripolskoj obshchnosti [Eustatic fluctuations of the Black Sea level and the dynamics of the development of the Cucuteni-Tripolye population]. Stratum Plus 2010 (2), 37–48.

Diachenko, A.V., 2012. Settlement system of West Tripolye culture in the Southern Bug and Dnieper Interfluve: formation problems. In: Menotti, F., Korvin-Piotrovskiy, A.G. (Eds.), The Tripolye Culture Giant-Settlements in Ukraine: Formation, Development, and Decline. Oxbow Books, Oxford, pp. 116–138.

Dolukhanov, P.M., Shukurov, A., Davison, K., Sarson, G., Gerasimenko, N.P., Pashkevich, G.A., Vybornov, A.A., Kovalyukh, N.N., Skripkin, V.V., Zaitseva, G.I., Sapelko, T.V., 2009. The sporead of Neolithic in the south east European plain: radiocarbon chronology, subsistence, and environment. Radiocarbon 51 (2), 783–793.

Farcas, S., de Beaulieu, J.L., Reille, M., Coldea, G., Diaconeasa, B., Goeury, C., Goslar, T., Jull, T., 1999. First ^{14}C datings of Late Glacial and Holocene pollen sequences from Romanian Carpathes. C. R. Acad. Sci. III 322, 799–807.

Farcas, S., Lupsa, V., Tantau, I., Bodnariuc, A., 2003. (in Romanian) Reflectarea procesului de antropizare în diagramele sporo-polinice din Muntii Apuseni [Reflections of human intervention in spore and pollen diagrams in the Apuseni Mountains]. Environ. Prog. 1, 231–236.

Feurdean, A., Bennike, O., 2004. Late Quaternary palaeoecological and palaeoclimatological reconstruction in the Gutaiului Mountains, northwest Romania. J. Quat. Sci. 19 (8), 808–827.

Filipova, M., 1985. Palaeoecological investigations of lake Shabla-Ezeretz in Northeastern Bulgaria. Ecol. Mediterr. 11 (1), 148–158.

Folland, C.K., Karl, T., Vinnikov, K.Ya., 1990. Observed climate variations and change. In: Houghton, J.T., Jenkins, G.J., Ephraums, J.J. (Eds.), Climate Change: The IPCC Scientific Assessment. Cambridge University Press, Cambridge, pp. 195–238.

Giosan, L., Donnelly, J.P., Constantinescu, S., Filip, F., Ovejanu, I., Vespremeanu-Stroe, A., Vespremeanu, E., Duller, G.A.T., 2006. Young Danube delta documents stable Black Sea level since middle Holocene: morphodynamic, paleogeographic, and archaeological implications. Geology 34 (9), 757–760.

Grindean, R., Tantau, I., Farcas, S., Panait, A., 2014. Middle to Late Holocene vegetation shifts in the NW Transylvanian lowlands (Romania). Studia UBB Geologia 59 (1), 29–37.

Hammer, Ø., 2016. PAST. https://folk.uio.no/ohammer/past/ accessed 08.02.16.

Harper, T.K., 2013. The effect of climatic variability on population dynamics of the Cucuteni-Tripolye cultural complex and the rise of the Western Tripolye giant-settlements. Chronika 3, 28–46.

Harper, T.K., 2016. *Climate, migration, and false cities on the Old European periphery: a*

spatial-demographic approach to understanding the Tripolye giant-settlements. Ph.D.dissertation, Department of Anthropology, State University of New York at Buffalo. Proquest, Ann Arbor, MI.
Jochim, M., 2011. The Mesolithic. In: Milisauskas, S. (Ed.), European Prehistory: A Survey. Springer, New York, pp. 125–152.
Joerin, U.E., Stocker, T.F., Schlüchter, C., 2006. Multicentury glacier fluctuations in the Swiss Alps during the Holocene. The Holocene 16 (5), 697–704.
Kremenetski, C.V., 1995. Holocene vegetation and climate history of southwestern Ukraine. Rev. Palaeobot. Palynol. 85, 289–301.
Lazarovici, G., 1987. (in Romanian) „Şocul" Vinča C în Transilvania [The Vinča C "shock" in Transylvania]. Acta Musei Porolissensis 11, 37–38.
Loper, S., 2012. Wheat growth stages in relation to management practices. University of Arizona Cooperative Extension presentation, 19–20 September 2012. https://cals.arizona.edu/crop/presentations/2012/ShawnaLoper.pdf accessed 07.03.16.
Mantu, C.-M., 1998. (in Romanian) Cultura Cucuteni: Evoluție, Cronologie, Legături [The Cucuteni Culture: Evolution, Chronology, Connections]. Muzeul de Istorie Piatra Neamț, Piatra Neamț.
Manzura, I., 2005. Steps to the steppe: or, how the North Pontic Region was colonised. Oxf. J. Archaeol. 24 (4), 313–338.
Mayewski, P.A., Meeker, L.D., Twickler, M.S., Whitlow, S.I., Yang, Q., Lyons, W.B., Prentice, M., 1997. Major features and forcing of high-latitude northern hemisphere atmospheric circulation using a 110,000-year-long glaciochemical series. J. Geophys. Res. 102, 26345–26366.
Mayewski, P.A., Rohling, E.E., Stager, J.C., Karlen, W., Maascha, K.A., Meeker, L.D., Meyerson, E.A., Gasse, F., van Kreveld, S., Holmgrend, K., Lee-Thorph, J., Rosqvist, G., Racki, F., Staubwasser, M., Schneider, R.R., Steig, E.J., 2004. Holocene climate variability. Quat. Res. 62, 243–255.
Miller, P., Lanier, W., Brandt, S., 2001. Using Growing Degree Days to Predict Plant Stages. Montana State University Extension Service Publication MT200103 AG 7/2001.
Mitchell, T.D., Jones, P.D., 2005. An improved method of constructing a database of monthly climate observations and associated high-resolution grids. Int. J. Climatol. 25, 693–712.
Mitchell, T.D., Carter, T.R., Jones, P.D., Hulme, M., New, M., 2004. A comprehensive set of high-resolution grids of monthly climate for Europe and the globe: the observed record (1901–2000) and 16 scenarios (2001–2100). Tyndall Centre Working Paper No. 5. Climate Research Unit, University of East Anglia.
Nakagawa, T., 2016. Computer programs produced by Takeshi Nakagawa. http://polsystems.rits-palaeo.com/ accessed 10.03.17.
Nakagawa, T., Tarasov, P.E., Nishida, K., Gotanda, K., Yasuda, Y., 2002. Quantitative pollen-based climate reconstruction in central Japan: application to surface and Late Quaternary spectra. Quat. Sci. Rev. 21, 2099–2113.
NDAWN (North Dakota Agricultural Weather Network), 2002. Wheat Growth Stage Prediction Using Growing Degree Days (GDD). https://ndawn.ndsu.nodak.edu/help-wheat-growing-degree-days.html accessed 07.03.16.
North Greenland Ice Core Project members (NGRIP), 2004. North Greenland Ice Core Project Oxygen Isotope Data. IGBP PAGES/World Data Center for Paleoclimatology Data Contribution Series #2004-059 NOAA/NGDC Paleoclimatology Program, Boulder CO, USA.
Pashkevich, G.O., Videjko, M.Yu., 2006. (in Ukrainian) *Rilnytsvo plemen Trypilskoyi kultury* [Crops of the Tripolye-culture Tribes]. Institute of Archaeology of the National Academy of Sciences of Ukraine, Kiev.
Peyron, O., Guiot, J., Cheddadi, R., Tarasov, P., Reille, M., de Beaulieu, J.-L., Bottema, S., Andrieu, V., 1998. Climatic reconstruction in Europe for 18,000 yr B.P. From pollen data. Quat. Res. 49, 183–196.
Prentice, I.C., Guiot, J., Huntley, B., Jolly, D., Cheddadi, R., 1996. Reconstructing biomes from palaeoecological data: a general method and its application to European pollen data at 0 and 6 ka. Clim. Dyn. 12, 185–194.
Rahmstorf, S., Box, J.E., Feulner, G., Mann, M.E., Robinson, A., Rutherford, S., Schaffernicht, E.J., 2015. Exceptional twentieth-century slowdown in Atlantic Ocean overturning circulation. Nat. Clim. Chang. 5, 475–480.
Reimer, P.J., Bard, E., Bayliss, A., Beck, J.W., Blackwell, P.G., Bronk Ramsey, C., Buck, C.E., Cheng, H., Edwards, R.L., Friedrich, M., Grootes, P.M., Guilderson, T.P., Haflidason, H., Hajdas, I., Hatté, C., Heaton, T.J., Hoffmann, D.L., Hogg, A.G., Hughen, K.A., Kaiser, K.F., Kromer, B., Manning, S.W., Niu, M., Reimer, R.W., Richards, D.A., Scott, E.M., Southon, J.R., Staff, R.A., Turney, C.S.M., van der Plicht, J., 2013. IntCal13 and Marine13 radiocarbon age calibration curves 0–50.000 cal BP. Radiocarbon 55 (4), 1869–1887.
Rohling, E.J., Mayewski, P.A., Abu-Zied, R.H., Casford, J.S.L., Hayes, A., 2002. Holocene atmosphere-ocean interactions: records from Greenland and the Aegean Sea. Clim. Dyn. 18, 587–593.
Rösch, M., Fischer, E., 2000. A radiocarbon dated Holocene pollen profile from the Banat mountains (Southwestern Carpathians, Romania). Flora 195, 277–286.
Ryzhov, S.M., 1993. (in Ukrainian) Nebelivska grupa pamyatok trypilskoyi kultury [The Nebelevskaya group of the Tripolye culture]. Arkheologiya 1993 (3), 101–114.
Ryzhov, S.M., 1999. (in Ukrainian) Keramika poselen trypilskoyi kultury Bugo-Dniprovskoho mezhyrichchya yak istorychne dzherelo [Ceramics of the Tripolye Culture Settlements of the Southern Bug and Dnieper Interfluve as an Archaeological Source]. Kandidat Nauk dissertation, Institut Arkheologii NAN Ukrainy, Kiev.
Ryzhov, S.M., 2007a. (in Ukrainian) Suchasniy stan vyvchennya kulturno-istorychnoyi spilnosti Kukuten-Trypillya na teritoriyi Ukrayiny [Recent understanding of the Cucuteni-Tripolye cultural complex in the territory of Ukraine]. In: Ryzhov, S.M., Rassamakin, Yu Ya (Eds.), O. Olzhych. Arkheologiya. Olena Teliga, Kiev, pp. 437–477.
Ryzhov, S.M., 2007b. (in Ukrainian) Vplyv shypynetskoyi lokalnoyi grupy na formuvannya pamyatok nebelivskoyi grupy u Bugo-Dniprovskomu mezhyrichchi [The impact of the Shypenetskaya local group on the formation of Nebelevskaya sites in the Bug-Dnieper interfluve]. ZNTSH. Pratsi Arkheologichnoyi komisiyi 253, 127–139.
Schneider, T., Bischoff, T., Haug, G.H., 2014. Migrations and dynamics of the intertropical convergence zone. Nature 513, 45–53.
Sirocko, F., Seelos, K., Schaber, K., Rein, B., Dreher, F., Diehl, M., Lehne, R., Jäger, K., Krbetschek, M., Degering, D., 2005. A late Eemian aridity pulse in central Europe during the last glacial inception. Nature 436, 833–836.
Spinoni, J., Barbosa, P., Vogt, J., 2015. European degree-day climatologies and trends for the period of 1951–2011. Int. J. Climatol. 35, 25–36. http://dx.doi.org/10.1002/joc.3959.
Tantau, I., 2003. Pollen analytic researches in the Eastern Romanian Carpathians. In: History of Vegetation and Human Impact. Thesis of Environmental Sciences, Paleontology and Stratigraphy. Aix-Marseille III University and Babes-Bolyai of Cluj-Napoca University.
Tarasov, P.E., Webb, T., Andreev, A.A., Afanas'eva, N.B., Berezina, N.A., Bezusko, L.G., Blyakharchuk, T.A., Bolikhovskaya, N.S., Cheddadi, R., Chernavskaya, M.M., Chernova, G.M., Dorofeyuk, N.I., Dirksen, V.G., Elina, G.A., Filimonova, L.V., Glebov, F.Z., Guiot, J., Gunova, V.S., Osipova, I.M., Panova, N.K., Prentice, I.C., Saarse, L., Sevastyanov, D.V., Volkova, V.S., Zernitskaya, V.P., 1998. Present-day and mid-Holocene biomes reconstructed from pollen and plant macrofossil data from the former Soviet Union and Mongolia. J. Biogeogr. 25, 1029–1053.
Waters, C.N., Zalasiewicz, J., Summerhayes, C., Barnosky, A.D., Poirier, C., Gałuszka, A., Cearreta, A., Edgeworth, M., Ellis, E.C., Ellis, M., Jeandel, C., Leinfelder, R., MacNeill, J.R., Richter, D.deB., Steffen, W., Syvitski, J., Vidas, D., Wagreich, M., Williams, M., Zhisheng, A., Grinevald, J., Odada, E., Oreskes, N., Wolfe, A.P., 2016. The Anthropocene is functionally and stratigraphically distinct from the Holocene. Science 351 (6269), aad2622.
Welten, M., 1982. (in German) *Vegetationsgeschichtliche Untersuchungen in den westlichen Schweizer Alpen: Bern-Wallis* [Vegetation History Studies in the Western Swiss Alps: Bern-Wallis]. Denkschriften der Schweizerischen Naturforschenden Gesellschaft 95. Birkhäuser, Basel.
Weninger, B., Harper, T., 2015. The geographic corridor for rapid climate change in Southeast Europe and Ukraine. In: Hansen, S., Raczky, P., Anders, A., Reingruber, A. (Eds.), Neolithic and Copper Age Between the Carpathians and the Aegean Sea: Chronologies and Technologies From the 6th to the 4th Millennium BCE. Archäologie in Eurasien 31. Deutsches Archäologisches Institut, Berlin, pp. 475–505.
Weninger, B., Alram-Stern, E., Bauer, E., Clare, L., Danzeglocke, U., Jöris, O., Kubatzki, C., Rollefson, G., Todorova, H., van Andel, T., 2006. Climate forcing due to the 8200 cal yr BP event observed at Early Neolithic sites in the eastern Mediterranean. Quat. Res. 66 (3), 401–420.
Weninger, B., Clare, L., Rohling, E.J., Bar-Yosef, O., Böhner, U., Budja, M., Bundschuh, M., Feurdean, A., Gebel, H.-G., Jöris, O., Linstädter, J., Mayewski, P., Mühlenbruch, T., Reingruber, A., Rollefson, G., Schyle, D., Thissen, L., Todorova, H., Zielhofer, C., 2009. The impact of rapid climate change on prehistoric societies during the Holocene in the Eastern Mediterranean. Documenta Praehistorica 36, 7–59.